

Indole Naphthyridinones as Inhibitors of Bacterial Enoyl-ACP Reductases FabI and FabK

Mark A. Seefeld,^{*,†} William H. Miller,[†] Kenneth A. Newlander,[†] Walter J. Burgess,[†] Walter E. DeWolf Jr.,[‡] Patricia A. Elkins,[§] Martha S. Head,[§] Dalia R. Jakas,[†] Cheryl A. Janson,[§] Paul M. Keller,[‡] Peter J. Manley,^{†,⊥} Terrance D. Moore,[#] David J. Payne,[#] Stewart Pearson,[#] Brian J. Polizzi,[‡] Xiayang Qiu,^{§,||} Stephen F. Rittenhouse,[#] Irene N. Uzinskas,[†] Nicola G. Wallis,^{#,⊗} and William F. Huffman[†]

GlaxoSmithKline Pharmaceuticals, 1250 South Collegeville Road, P.O. Box 5089, Collegeville, Pennsylvania 19426

Received September 13, 2002

Bacterial enoyl-ACP reductase (FabI) is responsible for catalyzing the final step of bacterial fatty acid biosynthesis and is an attractive target for the development of novel antibacterial agents. Previously we reported the development of FabI inhibitor **4** with narrow spectrum antimicrobial activity and in vivo efficacy against *Staphylococcus aureus* via intraperitoneal (ip) administration. Through iterative medicinal chemistry aided by X-ray crystal structure analysis, a new series of inhibitors has been developed with greatly increased potency against FabI-containing organisms. Several of these new inhibitors have potent antibacterial activity against multidrug resistant strains of *S. aureus*, and compound **30** demonstrates exceptional oral (po) in vivo efficacy in a *S. aureus* infection model in rats. While optimizing FabI inhibitory activity, compounds **29** and **30** were identified as having low micromolar FabK inhibitory activity, thereby increasing the antimicrobial spectrum of these compounds to include the FabK-containing pathogens *Streptococcus pneumoniae* and *Enterococcus faecalis*. The results described herein support the hypothesis that bacterial enoyl-ACP reductases are valid targets for antibacterial agents.

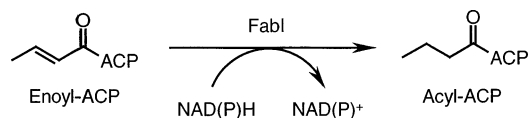
Introduction

Antibiotic resistant pathogens are a source of universal healthcare concern.^{1–3} Methicillin-resistant *Staphylococcus aureus* (MRSA) and vancomycin-resistant Enterococci (VRE) have become particularly troublesome as our remaining therapeutic defenses against these pathogens become progressively less effective. With the recent emergence of vancomycin-resistant *Staphylococcus aureus*,⁴ the need for new antibiotics is of paramount importance. A potential strategy for combating antibiotic resistance is to target novel mechanisms of action. One such approach is the inhibition of enzymes involved in bacterial fatty acid biosynthesis (FAB).^{5–7}

Fatty acid biosynthesis in bacteria is essential to the production of a number of lipid-containing components including the cell membrane. The bacterial fatty acid synthase system (FASII) utilizes discrete monofunctional enzymes that operate in conjunction with acyl carrier protein (ACP)-associated substrates. Mammalian fatty acid synthase (FASI) differs from FASII in that lipid biosynthesis is mediated by a single multifunctional enzyme-ACP complex. The differences in prokaryote and eukaryote fatty acid biosynthesis offer an attractive opportunity for selective FASII inhibition.

FabI is an enoyl-ACP reductase that catalyzes the ultimate and rate-limiting step of the chain elongation

Scheme 1. FabI Biosynthetic Reaction



process of FASII.⁸ The reaction involves the conjugate reduction of an enoyl-ACP to the corresponding acyl-ACP using the cofactor NAD(P)H as a hydride source (Scheme 1).^{9,10} Reports describing the antibacterial agents isoniazid,¹¹ diazaboranes,^{12–14} and triclosan (**1**)^{15–18} as inhibitors of bacterial enoyl-ACP reductase support a FabI-targeted approach to antibacterial drug therapy. However, recent studies have shown that other bacterial enoyl-ACP reductases exist in addition to FabI. A triclosan-resistant flavoprotein, termed FabK, has been shown to be the only enoyl ACP-reductase in *Streptococcus pneumoniae* and to exist together with FabI in *Enterococcus faecalis* and *Pseudomonas aeruginosa*.¹⁹ A third enoyl-reductase, FabL, is present along with FabI in *Bacillus subtilis*.²⁰ Therefore, an inhibitor designed to selectively target a single bacterial enoyl-ACP reductase would be expected to have a narrow spectrum of antimicrobial activity, whereas an inhibitor targeting multiple enoyl ACP-reductases should have a broader spectrum of activity.

In previous communications we described two series of small molecule-FabI inhibitors, exemplified by compounds **2**²¹ and **3**,²² that were optimized from screening leads obtained from the GlaxoSmithKline compound collection. Additional research from these labs led to the discovery of an aminopyridine-based FabI inhibitor **4**²³ that exhibits in vivo efficacy against *S. aureus* (Figure 1). We now report the discovery of a naphthyridinone-based series of FabI inhibitors that demonstrates im-

* To whom correspondence should be addressed. GlaxoSmithKline Pharmaceuticals, 1250 S. Collegeville Road, P.O. Box 5089, Collegeville, PA 19426. Phone: (610) 917-7936. Fax: (610) 917-4206. E-mail: Mark_A_Seefeld@gsk.com.

[†] Department of Medicinal Chemistry.

[‡] Department of Microbial Biochemistry.

[§] Department of Computational, Analytical & Structural Sciences.

[#] Department of Microbial Genetics.

[⊥] Current address: Merck Research Laboratories, West Point, PA.

^{||} Current Address: Pfizer Inc., Groton, CT.

[⊗] Current Address: Astex Technology, Cambridge, UK.

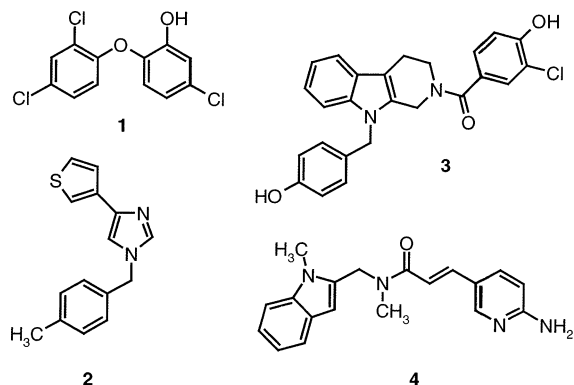


Figure 1. Small molecule FabI inhibitors.

Table 1. FabI Inhibition and Antibacterial Activity

Cmp.	R	IC ₅₀ (uM)		MIC (ug/mL)	
		<i>S. a.</i>	<i>H. inf.</i>	<i>S. a.</i> ^a	<i>H. inf.</i> ^b
4		2.4 ±1.2	4.2 ±1.1	0.5	>64
5		0.91 ±0.02	6.1 ±3.0	0.25	>64
11		2.3 ±0.65	2.7 ±0.1	0.5	>64
12		0.30 ±0.02	1.3 ±0.1	0.12	32
13		0.94 ±0.11	7.6 ±0.9	2.0	>64
21		0.05 ±0.01	0.56 ±0.17	0.03	32

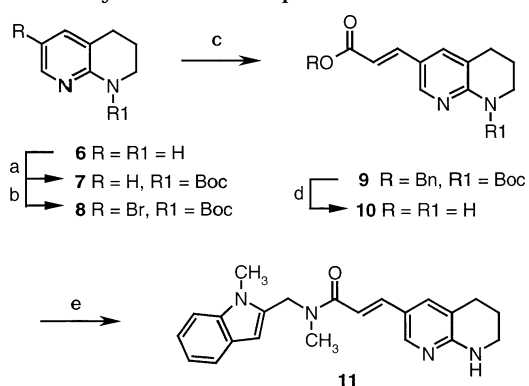
^a *S. aureus* WCUH29. ^b *H. influenzae* Q1.

improvements in potency, spectrum, and in vivo efficacy over previously reported selective FASII inhibitors. Significantly, selected compounds from this novel class of inhibitors display dual FabI/FabK inhibition.

Chemistry

Aminopyridines **4** and **5** (Table 1) were synthesized from commercially available reagents using procedures described in the literature.²³ Piperidine **11** was prepared similarly, as illustrated in Scheme 2, and exemplifies the method. 1,2,3,4-Tetrahydro-1,8-naphthyridine **6** was reacted under basic conditions with di-*tert*-butyl dicarbonate to give the Boc-protected intermediate **7**. Bromination using NBS in acetic acid followed by a Heck coupling²⁴ with benzyl acrylate provided compound **9**. Amine deprotection was accomplished under acidic conditions, and the benzyl ester was saponified in situ with LiOH. The resulting carboxylic acid **10** was coupled to 1-methyl-2-(methylaminomethyl)indole²³ in the presence of EDC to give the target compound **11**. Acetamido

Scheme 2. Synthesis of Compound 11^a



^a Reagents: (a) (Boc)₂O, THF, LiHMDS (76%); (b) NBS, HOAc (98%); (c) benzyl acrylate, Pd(OAc)₂, P(tolyl)₃, *i*-Pr₂NEt, CH₃CH₂CN, 90 °C (54%); (d) HCl in dioxane, then LiOH (29%); (e) EDC, HOBt, Et₃N, 1-methyl-2-(methylaminomethyl)indole, DMF (70%).

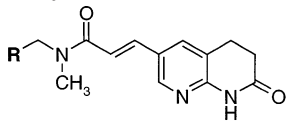
derivatives **12** and **13** were prepared by heating compounds **4** and **5**, respectively, with acetic anhydride.

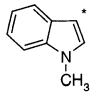
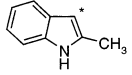
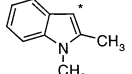
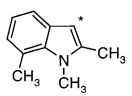
The naphthyridinone analogues **21** (Table 1) and **29–32** (Table 2) were prepared using the previously described method or as shown in Scheme 3. 2-Amino-3-hydroxymethylpyridine **14**,²⁵ prepared in two steps from 2-aminonicotinic acid, was reacted with bromine in acetic acid followed by HBr to give the crude dibromo intermediate **16**. Reaction of **16** with dimethyl malonate and sodium methoxide produced the expected malonate ester which cyclized under the reaction conditions to form the α -carboxymethyl naphthyridinone derivative **17**. The crude product was saponified with sodium hydroxide and then heated with 1 N HCl to afford pure bromo naphthyridinone **18**. A Heck coupling of **18** with *tert*-butyl acrylate and subsequent *tert*-butyl cleavage under standard acidic conditions gave acrylic acid **20**. Coupling of 1-methyl-2-(methylaminomethyl)indole with **20** using EDC produced the desired indole naphthyridinone **21**.

The indole amines **25–28** required for the production of target compounds **29–32** were synthesized by reductive amination using methylamine and an appropriate indole carboxaldehyde. The requisite indole carboxaldehydes were either obtained commercially or synthesized as described in Scheme 4. The preparation of indole **25** is representative. 2-Methylindole (**22**) was *N*-methylated with NaH and methyl iodide affording **23** in near quantitative yield. Subjecting 1,2-dimethylindole (**23**) to Vilsmeier reaction conditions²⁶ gave the aldehyde **24**. Reductive amination with methylamine and sodium borohydride in ethanol provided amine **25**.

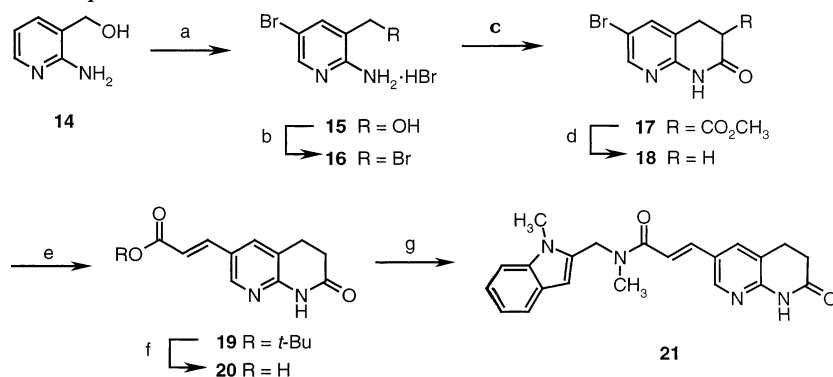
Results and Discussion

Compound **4**²³ has moderate activity against FabI from *S. aureus* (IC₅₀ = 2.4 μ M, apparent K_i = 0.21 \pm 0.11 μ M²⁷) and *Haemophilus influenzae* (IC₅₀ = 4.2 μ M, Table 1). Corresponding whole cell antibacterial activity was observed against *S. aureus* (MIC = 0.5 μ g/mL); however, none was detected against *H. influenzae* (MIC >64 μ g/mL). Additionally, **4** had no inhibitory effect on FabK (IC₅₀ >30 μ M), and this presumably explains the negligible antimicrobial activity against the FabK-containing organisms *E. faecalis* and *S. pneumoniae* (MICs >64 μ g/mL). The limited spectrum and potency of **4** was offset by impressive selectivity characteristics

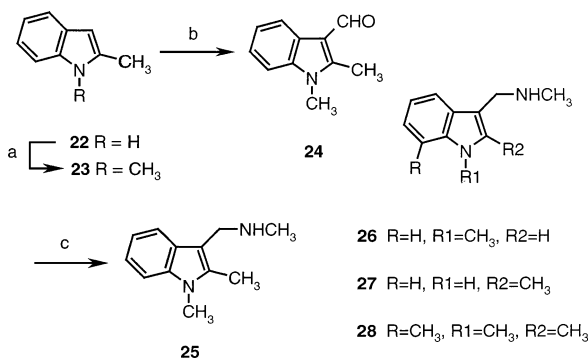
Table 2. FabI, FabK Inhibition and Antibacterial Activity


Cmp.	R	FabI IC ₅₀ (uM)			FabK IC ₅₀ (uM)		MIC (ug/mL)				
		<i>S. aureus</i>	<i>H. inf.</i>	<i>E. coli</i>	<i>S. pneum.</i>	<i>S. aureus</i> ^a	<i>H. inf.</i> ^b	<i>E. coli</i> ^c	<i>S. pneum.</i> ^d	<i>E. faec.</i> ^e	<i>M. cat.</i> ^f
29		0.13 ±0.03	0.39 ±0.06	0.07	5.0 ± 5.3	0.06	16	8	16	16	≤0.06
30		0.05 ±0.03	0.13 ±0.02	<0.06	3.0 ± 1.1	0.016	1	0.5	16	16	≤0.06
31		0.06 ±0.006	0.025 ±0.002	0.03 ±0.005	>30	≤0.001	>64	32	>64	>64	≤0.06
32		0.02 ±0.02	0.07 ±0.004	<0.07	>30	≤0.001	>64	>64	>64	>64	2
1	Triclosan	0.07 ±0.05	NT	0.43 ±0.40	>30	0.03	0.5	0.5	16	16	≤0.06

^a *S. aureus* WCUH29. ^b *H. influenzae* Q1. ^c *E. coli* 120AcrAB-. ^d *S. pneumoniae* 1629. ^e *E. faecalis* I. ^f *M. catarrhalis* 1502.

Scheme 3. Synthesis of Compound **21**^a

^a Reagents: (a) Br₂, HOAc (75%); (b) 48% HBr; (c) NaOCH₃, dimethyl malonate, CH₃OH (83% for two steps); (d) NaOH, CH₃OH, then HCl (88%); (e) *tert*-butyl acrylate, Pd(OAc)₂, P(tolyl)₃, DIEA, DMF, 90 °C (45%); (f) TFA, CH₂Cl₂ (100%); (g) EDC, HOBT, Et₃N, 1-methyl-2-(methylaminomethyl)indole, DMF (88%).

Scheme 4. General Synthesis of Indole Amines **25–28**^a

^a Reagents: (a) NaH, CH₃I, DMF, 0 °C (97%); (b) POCl₃, DMF (91%); (c) CH₃NH₂ in CH₃OH, then NaBH₄, EtOH (52%).

against the human FASI enzyme (IC₅₀ >100 uM). Furthermore, cytotoxicity (IC₅₀ = 512 μg/mL, in human A549 lung cells) and general cell membrane disruption (IC₅₀ = 630 uM in a liposome lysis assay) are not issues. The FabI inhibitor **4** was also efficacious *in vivo* against

S. aureus. Subsequent lead optimization studies were pursued with the goal of (a) increasing the potency of FabI inhibition, (b) expanding the spectrum of activity, and (c) increasing the level of efficacy *in vivo*.

The SAR depicted in Figure 2 shows the key pharmacophoric elements required for selective FabI inhibition in this series. A bicyclic aromatic structure, preferably indole, is linked at the 2' or 3' position to a methylamide via a methylene linker. The amide functionality is connected to the 5-position of a 2-aminopyridine through an (*E*)-olefin. Substitution on the indole moiety is limited to small lipophilic functionality, and substitution on the olefin results in a loss of enzyme inhibitory activity. The most accessible site for further chemical manipulation on the aminopyridine moiety is at the 3-position, and this is where we began our optimization studies.

The preferred substituents at the 3-position were found to be lipophilic and sterically undemanding (data not shown). Compound **5**, containing a 3-methyl substituent, showed increased potency toward *S. aureus*

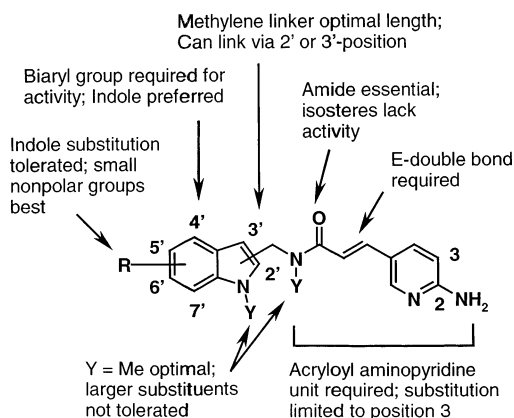


Figure 2. Aminopyridine FabI SAR.

(Table 1). Bridging the 3-methyl group to the adjacent amine functionality through a piperidine ring gave **11** which offered little improvement in enzyme potency or in vitro activity over the parent compound **4**, although it indicated that substitution on the amino group could be tolerated. N-Acylation of the exocyclic amine of **4** provided acetamido compound **12** and a severalfold increase in potency with a concomitant decrease in MIC for *S. aureus* and *H. influenzae*. Combining lipophilic substitution at position 3 with the *N*-acyl component of **12** provided no additive increase in potency for amide **13**. This result may be a consequence of the terminal amide having to adopt a suboptimal active-site conformation with an adjacent methyl substituent present. To test this hypothesis, the functionality at positions 2 and 3 of compound **13** were connected through the conformational constraint of a six-membered ring. The resulting compound, naphthyridinone **21**, was found to be a potent FabI inhibitor (IC_{50} , *S. aureus* = 0.05 μ M, apparent K_i = 4.3 ± 0.01 nM,²⁷ IC_{50} , *H. influenzae* = 0.56 μ M) with good antibacterial activity (MIC, *S. aureus* = 0.03 μ g/mL, *H. influenzae* = 32 μ g/mL). Compound **21** and the other compounds in Table 1 had no measurable activity against FabK.

We next turned our intention to the indole (left-hand) portion of **21** keeping the acryloyl naphthyridinone (right-hand) side of the molecule constant (Table 2). The preferred substituents on this portion of the inhibitor were also small and lipophilic with methyl substitution being representative. Changing the position of attachment from the 2'-linking position of **21** to the 3'-position of **29** had little effect on the level of FabI inhibition (*S. aureus*, *H. influenzae*, *E. coli*).²⁸ However, **29** was found to have antibacterial activity against the two FabK-containing organisms (*S. pneumoniae* MIC = 16 μ g/mL and *E. faecalis* MIC = 16 μ g/mL), and this was reflected in the *S. pneumoniae* FabK enzyme assay (FabK IC_{50} = 5 μ M). FabK inhibition was slightly improved by shifting the methyl group of **29** from N-1' to the adjacent 2'-position in **30** (*S. pneumoniae* FabK IC_{50} = 3 μ M). The addition of a second methyl group to **30** at position N-1' gave compound **31**, which had an IC_{50} >30 μ M against FabK and lost antibacterial activity against the FabK-containing organisms (*S. pneumoniae* MIC >64 μ g/mL, *E. faecalis* MIC >64 μ g/mL). Nonetheless, **31** had much improved antibacterial activity against *S. aureus* with MICs ≤ 0.001 μ g/mL. A similar result was obtained for the trimethyl analogue **32**, wherein enzyme potency

was maintained, but whole-cell activity was detected in only *S. aureus* and *M. catarrhalis*. It is interesting to note that the more heavily substituted indole compounds **31** and **32** are narrow-spectrum agents. The antibacterial activity against other organisms may be limited by efflux²⁹ or more probably cell penetration, since both **31** and **32** are potent inhibitors of *E. coli* FabI (0.03 μ M and 0.07 μ M, respectively), and both compounds have poor activity against the *E. coli* AcrAB-efflux mutant.

The enzyme activity of the naphthyridinone inhibitors is equipotent to that of triclosan (**1**), a known FabI inhibitor, but direct comparisons of IC_{50} s may not be valid. To achieve high levels of potency, triclosan undergoes a slow time-dependent formation of a stabilized complex with FabI and NAD^+ .^{30–32} There is no evidence that this new class of naphthyridinone inhibitors requires the formation of a similar complex to inhibit FabI.³³ Comparisons between the MICs of triclosan and the naphthyridinones are, however, quite valid. The majority of the naphthyridinones are more potent *S. aureus* inhibitors than triclosan. Furthermore, compounds **29** and **30** achieve a similar spectrum of antimicrobial activity to triclosan, but **29** and **30** have measurable FabK inhibition, whereas triclosan is not an inhibitor of FabK (IC_{50} >30 μ M). The activity of triclosan against FabK-containing organisms *S. pneumoniae* (MIC = 16 μ g/mL) and *E. faecalis* (MIC = 16 μ g/mL) suggests that triclosan may have additional mechanisms of action.^{34,35}

An X-ray cocrystallization study with naphthyridinone **29** (FabI *E. coli* IC_{50} = 0.07 μ M) and *E. coli* FabI- NAD^+ (Figure 3, bottom picture) reveals the key binding interactions. As expected, the binding characteristics of **29**³⁶ are quite similar to those previously described for compound **4**²² and for triclosan (Figure 3, top picture).³⁷ The linking amide carbonyl of **29** is well-positioned for an H-bond interaction with the 2'-hydroxyl of NAD^+ and the hydroxyl of tyrosine 156. The central *cis*-amide fragment of **29** appears to participate in a π -stacking interaction with the nicotinamide portion of NAD^+ as seen in **4**.²³ Alanine 95 is involved in H-bond interactions that bind both the pyridylamine and the *N*-acyl hydrogen of the naphthyridinone functionality. The contribution of the naphthyridinone carbonyl of **29** is not apparent in the crystal structure. The indole portion of inhibitor **29** is flanked by lipophilic residues (Met 206, Phe 203, Tyr 156, Tyr 146) creating tight hydrophobic packing. Substitution at indole sites other than 1', 2', and 7' of **29** would appear to create unfavorable steric interactions with neighboring backbone residues. Similar observations for other FabI inhibitors in this region of the active site have been described.^{14,23}

Recent studies have shown that a clinically relevant (F204C) mutation in the active site of *S. aureus* FabI (F203C in *E. coli*) negatively affects triclosan potency, but has no significant effect on the MIC of the naphthyridinone compounds.³³ We speculate that the binding orientation of naphthyridinone **29** in *S. aureus* positions the molecule away from the mutation site. In general, the antibacterial potency of the indole naphthyridinones remains relatively unaffected by the active-site mutations that confer susceptibility to triclosan.

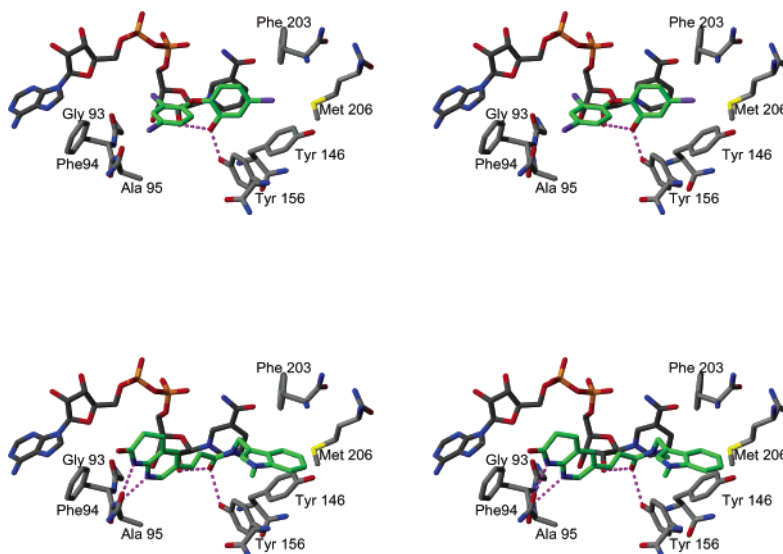


Figure 3. Representations of the X-ray crystal structures of triclosan (upper picture) and **29** (lower picture) bound to *E. coli* FabI–NAD⁺.

An extensive characterization of the biological activities of these compounds, and in particular compound **30**, has been discussed.²⁹ In summary, all naphthyridinones were tested against bacterial strains of over-expressing *S. aureus* and *H. influenzae* FabI and showed elevated MICs (>4-fold) versus WT strains. Additionally, all compounds were shown to selectively inhibit acetate incorporation in ¹⁴C-labeled precursor pathway macromolecular synthesis studies using *S. aureus*. The naphthyridinone inhibitors had no detectable activity against the human fatty acid biosynthetic enzyme (IC₅₀ > 100 μM) and showed no significant cytotoxicity (TC_{50s} > 64 μg/mL). Together, these studies support a mode of action (MOA) for these compounds as fatty acid synthesis (FASII) inhibitors.

A tertiary profile was run with selected naphthyridinones against a panel of clinical isolates of *S. aureus* that were resistant to different classes of currently available antibiotics. Several naphthyridinones displayed levels of inhibition better than marketed antibiotics, with compound **30** achieving MIC_{90s} > 500-fold lower than those exhibited by the commercial antibiotics tested. In in vivo studies, following oral administration at 50 mg/kg, **30** was found to be effective in a rat groin abscess model (infected with the MRSA strain WCUH 29), providing a 3.5-log reduction in bacterial counts relative to untreated controls.²⁹

Conclusion

A FabI inhibitor **4** with a narrow spectrum of antimicrobial activity and moderate target potency has been modified to produce a series of FabI inhibitors that exhibit potent activity against a panel of drug resistant strains of *S. aureus*. A representative compound, **30**, from this series displays excellent oral in vivo efficacy against *S. aureus* in rats. In addition, inhibitor **30** is a low micromolar inhibitor of FabK and thus as a dual FabI/FabK inhibitor has broad spectrum activity. The MIC profile for the systemically active compound **30** is comparable to triclosan. Subtle differences between the binding characteristics of triclosan and the indole naphthyridinone inhibitors suggest that these compounds

will be active against triclosan resistant strains. Mode of action and cytotoxicity studies have shown that the naphthyridinone compounds are selective FabI inhibitors with no detectable FASI inhibition. Further investigation into FabI and FabK inhibition in our laboratories is ongoing and will be reported on in due course.

Experimental Section

General. All starting materials were either purchased from commercial sources or reported previously in the literature unless otherwise noted. Solvents and reagents were used without further purification. Reactions were monitored by TLC on precoated silica gel plates (Kieselgel 60 F₂₅₄, Merck). Purification was performed by flash chromatography using silica gel (particle size 40–63 μm, Merck). Celite is a filter aid composed of acid-washed diatomaceous silica and is a registered trademark of Manville Corp., Denver, CO. ¹H NMR spectra were recorded on Bruker series spectrometers at the indicated field strengths. Chemical shifts are reported as ppm (δ) relative to TMS as an internal standard. Only major rotamer peaks are reported. Mass spectra were recorded on either Micromass or Sciex electrospray LC-MS spectrometers. Microanalysis was carried out by Quantitative Technologies, Inc., Whitehouse, NJ. HRMS was performed by the analytical department of GlaxoSmithKline Pharmaceuticals.

1-(tert-Butoxycarbonyl)-1,2,3,4-tetrahydro-1,8-naphthyridine (7). To a solution of 1,2,3,4-tetrahydro-1,8-naphthyridine (**6**) (1.04 g, 7.68 mmol) and di-*tert*-butyl dicarbonate (2.01 g, 9.22 mmol) in dry THF (40 mL) was added a solution of LiHMDS in THF (1.0 M, 9.22 mL, 9.22 mmol) dropwise at 0 °C. After 30 min the mixture was quenched with saturated NH₄Cl and extracted with EtOAc (2 × 200 mL). The combined organic layers were dried (MgSO₄), filtered, and concentrated. Flash chromatography on silica gel (40% EtOAc/hexanes) gave the title compound (1.37 g, 76%) as an orange oil which solidified under vacuum. ¹H NMR (400 MHz, CDCl₃) δ 8.33 (m, 1H), 7.37 (m, 1H), 6.94 (m, 1H), 3.77 (m, 2H), 2.75 (t, *J* = 6.5 Hz, 2H), 1.93 (m, 2H), 1.54 (s, 9H).

1-(tert-Butoxycarbonyl)-6-bromo-1,2,3,4-tetrahydro-1,8-naphthyridine (8). To a solution of 1-(*tert*-butoxycarbonyl)-1,2,3,4-tetrahydro-1,8-naphthyridine (**7**) (1.37 g, 5.85 mmol) in CH₂Cl₂ (30 mL) were added glacial HOAc (3.4 mL, 58.5 mmol) and NBS (1.09 g, 6.14 mmol). After 72 h the mixture was washed with 2 M NaOH, H₂O, and brine. The mixture was dried (MgSO₄), filtered, and concentrated under reduced pressure to give the title compound (1.79 g, 98%) which was used directly in the next step. ¹H NMR (400 MHz,

CDCl₃) δ 8.35 (s, 1H), 7.51 (s, 1H), 3.77 (m, 2H), 2.75 (t, J = 6.5 Hz, 2H), 1.93 (m, 2H), 1.54 (s, 9H).

Benzyl (*E*)-3-[8-(*tert*-butoxycarbonyl)-5,6,7,8-tetrahydro-1,8-naphthyridin-3-yl]acrylate (9**).** A solution of 1-(*tert*-butoxycarbonyl)-6-bromo-1,2,3,4-tetrahydro-1,8-naphthyridine (**8**) (1.79 g, 5.70 mmol), benzyl acrylate (1.11 g, 6.84 mmol), Pd(OAc)₂ (65 mg, 0.29 mmol), P(*o*-tolyl)₃ (173 mg, 0.57 mmol), and (*i*-Pr)₂NEt (2.5 mL, 14.25 mmol) in propionitrile (30 mL) was degassed (N₂) and then heated to reflux. After 18 h the mixture was cooled to RT, filtered through Celite, and concentrated. Flash chromatography on silica gel (25% EtOAc/hexanes) gave the title compound (1.21 g, 54%) as a yellow solid. ¹H NMR (400 MHz, CDCl₃) δ 8.44 (s, 1H), 7.65 (d, J = 16.0 Hz, 1H), 7.53 (s, 1H), 7.40 (m, 5H), 6.43 (d, J = 16.0 Hz, 1H), 5.25 (s, 2H), 3.77 (m, 2H), 2.75 (t, J = 6.5 Hz, 2H), 1.93 (m, 2H), 1.54 (s, 9H).

(*E*)-3-(5,6,7,8-Tetrahydro-1,8-naphthyridin-3-yl)acrylic Acid (10**).** Benzyl (*E*)-3-[8-(*tert*-butoxycarbonyl)-5,6,7,8-tetrahydro-1,8-naphthyridin-3-yl]acrylate (**9**) (1.21 g, 3.07 mmol) was dissolved in 4 N HCl in dioxane (15 mL). After 18 h the mixture was concentrated. The residue was taken up in 1:1 MeOH/H₂O (15 mL). LiOH (1 N) (15 mL, 15.0 mmol) was added and the mixture heated to reflux. After 18 h the mixture was cooled to RT and concentrated to approximately 1/3 volume. The mixture was adjusted to pH 6 using 10% HCl. The resulting solid was collected by filtration, washed with H₂O, and dried under vacuum to give the title compound (0.18 g, 29%). ¹H NMR (400 MHz, DMSO-*d*₆) δ 7.95 (s, 1H), 7.55 (s, 1H), 7.40 (d, J = 15.8 Hz, 1H), 7.13 (s, 1H), 6.17 (d, J = 15.8 Hz, 1H), 3.33 (m, 2H), 2.67 (t, J = 5.8 Hz, 2H), 1.77 (m, 2H). LCMS (ES) *m/e* 205 (M + H)⁺.

(*E*)-*N*-Methyl-*N*-(1-methyl-1*H*-indol-2-ylmethyl)-3-(5,6,7,8-tetrahydro-1,8-naphthyridin-3-yl)acrylamide (11**).** To a solution of (*E*)-3-(5,6,7,8-tetrahydro-1,8-naphthyridin-3-yl)acrylic acid (**10**) (0.18 g, 0.88 mmol), hydroxybenzotriazole monohydrate (0.13 g, 0.97 mmol), diisopropylethylamine (0.17 mL, 0.97 mmol), and 1-methyl-2-(methylaminomethyl)indole (0.17 g, 0.97 mmol) in DMF (50 mL) at RT was added EDC (0.19 g, 0.97 mmol). After 12 h the reaction solution was concentrated under vacuum, and the residue was purified by flash chromatography on silica gel (9:1 CHCl₃/CH₃OH containing 5% NH₄OH) to give the title compound (0.22 g, 70%) as a light yellow solid. ¹H NMR (400 MHz, DMSO-*d*₆) δ 7.99–6.82 (m, 8H), 6.40 (s, 1H), 4.82 (s, 2H), 3.67 (m, 2H), 3.29 (m, 3H), 3.07 (m, 3H), 2.73 (m, 2H), 1.77 (m, 2H). LCMS (ES) *m/e* 361 (M + H)⁺. HRMS (ES): calcd for C₂₂H₂₄N₄O 360.1948, found 360.1950.

2-Amino-5-bromo-3-(hydroxymethyl)pyridine (15**).** To a stirred solution of 2-amino-3-(hydroxymethyl)pyridine (**14**) (15.0 g, 121.0 mmol) in HOAc (300 mL) at RT was added bromine (6.2 mL, 121.0 mmol) dropwise over 1 h. A suspension formed after approximately 15 min. After the addition, the reaction was stirred for an additional 1 h, then was concentrated under vacuum. The residue was taken up in 1 M Na₂CO₃ (500 mL), and the solution was extracted with ethyl acetate (2 × 250 mL). The combined organic layers were washed with brine, dried (Na₂SO₄), and concentrated to dryness. The resulting residue was triturated with a small volume of petroleum ether, filtered, and dried under vacuum to give the title compound (18.45 g, 75%) as a beige solid. ¹H NMR (400 MHz, DMSO-*d*₆) δ 7.89 (d, J = 2.3 Hz, 1H), 7.52 (s, 1H), 5.92 (br s, 2H), 5.29 (br s, 1H), 4.30 (s, 2H). LCMS (ES) *m/e* 203 (M + H)⁺.

2-Amino-5-bromo-3-(bromomethyl)pyridine Hydrobromide (16**).** A solution of 2-amino-5-bromo-3-hydroxymethylpyridine (**15**) (18.45 g, 91.3 mmol) in 48% aqueous HBr (50 mL) was heated at reflux for 12 h. The reaction was concentrated, and toluene was used to azeotrope the residual H₂O. The resulting light brown solid was placed under high vacuum overnight and used directly.

Methyl (±)-6-Bromo-2-oxo-1,2,3,4-tetrahydro-1*H*-1,8-naphthyridine-3-carboxylate (17**).** To a solution of sodium methoxide (20.57 mL, 25wt % in CH₃OH) in CH₃OH (75 mL) was added dimethyl malonate (11.87 g, 89.9 mmol). After 30

min, crude 2-amino-5-bromo-3-(bromomethyl)pyridine hydrobromide (**16**) (7.80 g, 22.5 mmol) was added to the methoxide solution, and the reaction was stirred at RT overnight. The reaction slurry was concentrated to dryness under vacuum and then suspended in 1:1 H₂O/Et₂O. The remaining solids were filtered and washed with H₂O and then with hexanes to afford the title compound (5.34 g, 83%) as a white solid after drying. ¹H NMR (400 MHz, DMSO-*d*₆) δ 11.02 (br s, 1H), 8.24 (s, 1H), 7.91 (s, 1H), 3.79 (t, J = 8.0 Hz, 1H), 3.66 (s, 3H), 3.16 (d, J = 7.8 Hz, 2H). LCMS (ES) *m/e* 286 (M + H)⁺.

6-Bromo-3,4-dihydro-1*H*-1,8-naphthyridin-2-one (18**).** To a solution of methyl (±)-6-bromo-2-oxo-1,2,3,4-tetrahydro-1*H*-1,8-naphthyridine-3-carboxylate (**17**) (2.00 g, 7.0 mmol) in CH₃OH (75 mL) was added 1 M NaOH (30 mL). The reaction was heated to reflux for 4 h and then cooled to RT. The reaction was neutralized with 1 M HCl (30 mL) and heated at reflux overnight. The reaction slurry was concentrated to dryness and the residue was suspended in 95:5 CHCl₃/CH₃OH. The solids were removed by filtration, and the filtrate was concentrated to afford the title compound (1.40 g, 88%) as an off-white solid. ¹H NMR (400 MHz, DMSO-*d*₆) δ 10.60 (br s, 1H), 8.32 (s, 1H), 7.94 (s, 1H), 3.32 (app t, 3H), 2.97 (app t, 3H). LCMS (ES) *m/e* 228 (M + H)⁺. Anal. (C₈H₇N₂O₁Br) C, H, N.

***tert*-Butyl (*E*)-3-(7-Oxo-5,6,7,8-tetrahydro-1,8-naphthyridin-3-yl)acrylate (**19**).** A solution of 6-bromo-3,4-dihydro-1*H*-1,8-naphthyridin-2-one (**18**) (12.99 g, 57.0 mmol), *tert*-butyl acrylate (34 mL, 232 mmol), DIEA (21.2 mL, 122.0 mmol), Pd(OAc)₂ (1.3 g, 5.8 mmol), and P(*o*-tol)₃ (3.5 g, 11.5 mmol) in propionitrile (200 mL) and DMF (50 mL) was purged with Ar, then was heated at reflux. After 18 h the reaction was allowed to cool to room temperature, filtered through Celite, and then concentrated to dryness. The residue was purified by flash chromatography on silica gel (5% MeOH/CHCl₃). The resulting residue was triturated with 1:1 Et₂O/petroleum ether, collected, and dried to give the title compound (7.09 g, 45%) as an off-white solid. ¹H NMR (400 MHz, DMSO-*d*₆) δ 10.70 (s, 1H), 8.35 (d, J = 2.0 Hz, 1H), 8.04 (s, 1H), 7.50 (d, J = 16.0 Hz, 1H), 6.51 (d, J = 16.0 Hz, 1H), 2.89 (t, 2H), 2.53 (t, 2H), 1.48 (s, 9H). LCMS (ES) *m/e* 275 (M + H)⁺.

(*E*)-3-(7-Oxo-5,6,7,8-tetrahydro-1,8-naphthyridin-3-yl)acrylic Acid Hydrochloride Salt (20**).** *tert*-Butyl (*E*)-3-(7-oxo-5,6,7,8-tetrahydro-1,8-naphthyridin-3-yl)acrylate (**19**) (7.0 g, 25.5 mmol) was dissolved in 1:1 TFA/CH₂Cl₂ (100 mL). The reaction solution was stirred for 30 min and then concentrated under vacuum. The residue was suspended in 4 N HCl/dioxane (100 mL), triturated, and concentrated to dryness. The resulting solid was triturated with Et₂O, collected, and dried under vacuum to give the title compound (6.55 g, 100%) as a off-white solid: ¹H NMR (400 MHz, DMSO-*d*₆) δ 10.72 (s, 1H), 8.35 (d, J = 2.0 Hz, 1H), 8.04 (s, 1H), 7.54 (d, J = 16.0 Hz, 1H), 6.51 (d, J = 16.0 Hz, 1H), 2.91 (t, 2H), 2.53 (t, 2H). LCMS (ES) *m/e* 219.0 (M + H)⁺.

(*E*)-*N*-Methyl-*N*-(1-methyl-1*H*-indol-2-ylmethyl)-3-(7-oxo-5,6,7,8-tetrahydro-1,8-naphthyridin-3-yl)acrylamide (21**).** To a solution of (*E*)-3-(7-oxo-5,6,7,8-tetrahydro-1,8-naphthyridin-3-yl)acrylic acid hydrochloride salt (**20**) (0.53 g, 2.1 mmol), hydroxybenzotriazole monohydrate (0.31 g, 2.3 mmol), diisopropylethylamine (0.80 mL, 4.6 mmol), and 1-methyl-2-(methylaminomethyl)indole (0.40 g, 2.3 mmol) in DMF (50 mL) at RT was added EDC (0.46, 2.3 mmol). After 12 h the reaction solution was concentrated under vacuum, and the residue was purified by flash chromatography on silica gel (9:1 CHCl₃/CH₃OH containing 5% NH₄OH) to give the title compound (0.69 g, 88%) as a light yellow solid. ¹H NMR (400 MHz, DMSO-*d*₆) δ 10.67 (s, 1H), 8.38 (s, 1H), 8.09 (m, 1H), 7.55 (d, J = 15.4 Hz, 1H), 7.48–7.39 (m, 2H), 7.25 (m, 1H), 7.11 (m, 1H), 7.0 (m, 1H), 6.42 (s, 1H), 4.85 (s, 2H), 3.68 (s, 3H), 3.11 (s, 3H), 2.93 (m, 2H), 2.53 (m, 2H). MS (ES) *m/e* 375 (M + H)⁺. Anal. (C₂₂H₂₂N₄O₂·0.9 H₂O) C, H, N.

(E)-3-(6-Amino-5-methylpyridin-3-yl)-N-methyl-N-(1-methyl-1H-indol-2-ylmethyl)acrylamide (5). According to the procedure of compound **21**, except substituting 2-amino-5-bromo-3-methylpyridine (1.72 g, 10.0 mmol) for 6-bromo-3,4-dihydro-1H-1,8-naphthyridin-2-one (**18**), the title compound (1.65 g, 49% for three steps) was prepared as a light yellow solid. ¹H NMR (300 MHz, DMSO-*d*₆) δ 8.04 (d, 1H), 7.75 (d, 1H), 7.49 (d, *J* = 15.2 Hz, 1H), 7.45 (m, 2H), 7.15 (t, *J* = 7.5 Hz, 1H), 7.02 (m, 2H), 6.42 (s, 1H), 6.28 (m, 2H), 4.84 (s, 2H), 3.68 (s, 3H), 3.09 (s, 3H), 2.06 (s, 3H). LCMS (ES) *m/e* 335 (M + H)⁺. Anal. (C₂₀H₂₂N₄O₁·0.25 H₂O) C, H, N.

(E)-3-[6-Acetylamino]pyridin-3-yl]-N-methyl-N-(1-methyl-1H-indol-2-ylmethyl)acrylamide (12). To a solution of **4** (0.50 g, 1.56 mmol) and acetic anhydride (0.19 g, 1.87 mmol) in THF (75 mL) was added NaHCO₃ (0.17 g, 2.03 mmol). After 36 h at 60 °C with vigorous stirring, the reaction contents were concentrated under vacuum and partitioned between EtOAc and H₂O. The organic layer was separated, washed with brine, dried over Na₂SO₄, and concentrated. Trituration with diethyl ether and drying under high vacuum afforded **12** (0.55 g, 98%) as a white solid. ¹H NMR (300 MHz, DMSO-*d*₆) δ 10.69 (s, 1H), 8.63 (s, 1H), 8.19 (m, 2H), 7.58 (d, *J* = 11.5 Hz, 1H), 7.51–7.26 (m, 3H), 7.12 (m, 1H), 7.01 (m, 1H), 6.43 (s, 1H), 4.86 (s, 2H), 3.72 (s, 3H), 3.12 (s, 3H), 2.12 (s, 3H). LCMS (ES) *m/e* 363 (M + H)⁺. Anal. (C₂₁H₂₂N₄O₂) C, H, N.

(E)-3-[6-Acetylamino-5-methylpyridin-3-yl]-N-methyl-N-(1-methyl-1H-indol-2-ylmethyl)acrylamide (13). To a solution of **5** (0.47 g, 1.41 mmol) and acetic anhydride (0.29 g, 2.82 mmol) in THF (75 mL) was added NaHCO₃ (0.35 g, 4.22 mmol). After 50 h at 60 °C with vigorous stirring, the reaction contents were concentrated under vacuum and partitioned between EtOAc and H₂O. The organic layer was separated, washed with brine, dried over Na₂SO₄, and concentrated. Trituration with diethyl ether and drying under high vacuum afforded **13** (0.49 g, 93%) as a white solid. ¹H NMR (400 MHz, CDCl₃) δ 8.36 (s, 1H), 7.70 (m, 1H), 7.58 (d, *J* = 7.7 Hz, 1H), 7.25 (m, 2H), 7.11 (t, *J* = 7.5 Hz, 1H), 6.92 (d, *J* = 15.5 Hz, 1H), 6.50 (s, 1H), 4.86 (s, 2H), 3.72 (s, 3H), 3.12 (s, 3H), 2.29 (s, 3H), 2.10 (s, 3H). LCMS (ES) *m/e* 377 (M + H)⁺. Anal. (C₂₂H₂₄N₄O₂·1.25 H₂O) C, H, N.

1,2-Dimethyl-1H-indole (23). To a stirred solution of 2-methylindole (**22**) (15.0 g, 114.3 mmol) in dry DMF (200 mL) was added NaH (60% dispersion in oil, 5.0 g, 125.0 mmol) in portions. The mixture was stirred for 30 min, then iodomethane (8.0 mL, 129.0 mmol) was added in one portion. The reaction became exothermic and was cooled in an ice bath. After 16 h at RT, the reaction was concentrated under vacuum and the residue was taken up in ethyl acetate. The solution was washed with H₂O then with brine, dried (MgSO₄), and concentrated to dryness. Purification on silica gel (hexanes/EtOAc, 1:1) gave the title compound (16.10 g, 97%) as an off-white solid. ¹H NMR (400 MHz, CDCl₃) δ 7.49 (d, *J* = 8.0 Hz, 1H), 7.03–7.19 (m, 3H), 6.21 (s, 1H), 3.56 (s, 3H), 2.34 (s, 3H).

1,2-Dimethyl-1H-indole-3-carboxaldehyde (24). To a stirred solution of phosphorus oxychloride (7.0 mL, 75.0 mmol) in DMF (25 mL) was added dropwise a solution of 1,2-dimethyl-1H-indole (**23**) (12.0 g, 82.6 mmol) in dry DMF (6.0 mL). The reaction was stirred at RT for 2 h and then poured onto ice. The mixture was made basic with a solution of NaOH (13.2 g, 330 mmol) in H₂O (44 mL), then was extracted with Et₂O (2 × 50 mL). The combined organic layers were washed with brine, dried (MgSO₄), and concentrated under vacuum. Flash chromatography on silica gel (10% ethyl acetate/hexanes) gave the title compound (13.03 g, 91%) as an off-white solid. ¹H NMR (400 MHz, DMSO-*d*₆) δ 10.07 (s, 1H), 8.16 (d, *J* = 7.9 Hz, 1H), 7.54 (d, *J* = 7.6 Hz, 1H), 7.22 (m, 2H), 3.73 (s, 3H), 2.69 (s, 3H). LCMS (ES) *m/e* 174 (M + H)⁺.

1,2-Dimethyl-3-(methylaminomethyl)-1H-indole (25). To a solution of 1,2-dimethyl-1H-indole-3-carboxaldehyde (**24**) (13.0 g, 75.0 mmol) in MeOH (200 mL) was added a solution of 2.0 M CH₃NH₂ in MeOH (113 mL, 225.0 mmol). The reaction was stirred at RT for 3 h, then was concentrated to a light yellow oil. This oil was dissolved in EtOH (300 mL), and

NaBH₄ (2.84 g, 75.0 mmol) was added. After 6 h the reaction was concentrated to a slurry and dissolved in 1 N NaOH (75 mL). The aqueous solution was extracted with Et₂O (2 × 200 mL), and the combined organic fractions were dried over Na₂SO₄ and concentrated. Flash chromatography on silica gel (9:1 CHCl₃/MeOH containing 5% NH₄OH) and drying in high vacuum afforded the title compound (7.33 g, 52%) as a faintly yellow oil. ¹H NMR (400 MHz, CDCl₃) δ 7.60 (d, *J* = 7.7 Hz, 1H), 7.29 (d, *J* = 8.0 Hz, 1H), 7.19 (t, 1H), 7.12 (t, 1H), 3.93 (s, 2H), 3.69 (s, 3H), 2.49 (s, 3H), 2.45 (s, 3H).

1-Methyl-3-(methylaminomethyl)-1H-indole (26). According to the procedure for compound **25**, except substituting 1-methylindole-3-carboxaldehyde (10.0 g, 62.8 mmol) for 1,2-dimethylindole-3-carboxaldehyde (**24**), the title compound (10.1 g, 92%) was prepared as a faintly yellow oil. ¹H NMR (400 MHz, CDCl₃) δ 7.63 (d, *J* = 6.8 Hz, 1H), 7.29 (m, 1H), 7.21 (t, *J* = 6.4 Hz, 1H), 7.12 (t, *J* = 6.5 Hz, 1H), 6.95 (s, 1H), 3.90 (s, 2H), 3.71 (s, 3H), 2.48 (s, 3H). LCMS (ES) *m/e* 175 (M + H)⁺.

2-Methyl-3-(methylaminomethyl)indole (27). According to the procedure for compound **25**, except substituting 2-methylindole-3-carboxaldehyde (10.0 g, 62.8 mmol) for 1,2-dimethylindole-3-carboxaldehyde (**24**), the title compound (6.88 g, 63%) was prepared as a faintly yellow low-melting solid. ¹H NMR (400 MHz, CDCl₃) δ 7.96 (br s, 1H), 7.56 (d, *J* = 6.7 Hz, 1H), 7.27 (d, *J* = 6.4 Hz, 1H), 7.10 (m, 2H), 3.88 (s, 2H), 2.46 (s, 3H), 2.41 (s, 3H). LCMS (ES) *m/e* 175 (M + H)⁺.

3-(Methylaminomethyl)-1,2,7-trimethylindole (28). According to the procedure for compound **25**, except substituting 2,7-dimethylindole (1.14 g, 7.84 mmol) for the 2-methyl-1H-indole (**22**), the title compound (570 mg, 36% for three steps) was obtained as a light yellow oil which solidified upon standing. ¹H NMR (400 MHz, CDCl₃) δ 7.42 (d, *J* = 7.6 Hz, 1H), 6.96 (t, 1H), 6.87 (m, 1H), 3.97 (s, 3H), 3.88 (s, 2H), 2.80 (s, 3H), 2.49 (s, 3H), 2.41 (s, 3H). LC-MS (ES) *m/e* 405 (2M + H)⁺.

(E)-N-Methyl-N-(1-methyl-1H-indol-3-ylmethyl)-3-(7-oxo-5,6,7,8-tetrahydro-1,8-naphthyridin-3-yl)acrylamide (29). According to the procedure of compound **21**, except substituting 1-methyl-3-(methylaminomethyl)indole (**26**) (0.75 g, 3.3 mmol) for 1-methyl-2-(methylaminomethyl)indole, the title compound (0.59 g, 72%) was prepared as a light yellow solid. ¹H NMR (400 MHz, DMSO-*d*₆) δ 10.65 (s, 1H), 8.58 (s, 1H), 8.37 (s, 1H), 8.06 (m, 2H), 7.64–6.93 (m, 5H), 4.73 (s, 2H), 3.76 (s, 3H), 3.37 (s, 3H), 2.90 (m, 2H), 2.51 (m, 2H). MS (ES) *m/e* 375 (M + H)⁺. Anal. (C₂₂H₂₂N₄O₂·0.9H₂O) C, H, N.

(E)-N-Methyl-N-(2-methyl-1H-indol-3-ylmethyl)-3-(7-oxo-5,6,7,8-tetrahydro-1,8-naphthyridin-3-yl)acrylamide (30). According to the procedure of compound **21**, except substituting 2-methyl-3-(methylaminomethyl)indole (**27**) (1.40 g, 8.0 mmol) for 1-methyl-2-(methylaminomethyl)indole, the title compound (1.30 g, 65%) was prepared as a light yellow solid. ¹H NMR (400 MHz, DMSO-*d*₆) δ 10.91 (s, 1H), 10.64 (s, 1H), 8.36 (s, 1H), 8.06 (m, 1H), 7.53 (d, *J* = 15.4 Hz, 1H), 7.49 (m, 1H), 7.33–7.23 (m, 2H), 7.16 (d, *J* = 15.4 Hz, 1H), 6.97 (t, *J* = 7.5 Hz, 1H), 6.90 (t, *J* = 7.5 Hz, 1H), 4.74 (s, 2H), 2.96 (s, 3H), 2.89 (m, 2H), 2.52 (m, 2H), 2.42 (s, 3H). LCMS (ES) *m/e* 375 (M + H)⁺. Anal. (C₂₂H₂₂N₄O₂·0.9H₂O) C, H, N.

(E)-N-(1,2-Dimethyl-1H-indol-3-ylmethyl)-N-methyl-3-(7-oxo-5,6,7,8-tetrahydro-1,8-naphthyridin-3-yl)acrylamide (31). According to the procedure of compound **21**, except substituting 1,2-dimethyl-3-(methylaminomethyl)indole (**26**) (0.50 g, 2.66 mmol) for 1-methyl-2-(methylaminomethyl)indole, the title compound (0.74 g, 79%) was prepared as a light yellow solid. ¹H NMR (400 MHz, DMSO-*d*₆) δ 10.65 (s, 1H), 8.36 (s, 1H), 8.05 (m, 1H), 7.56 (m, 2H), 7.37 (m, 1H), 7.17 (d, *J* = 15.4 Hz, 1H), 7.07 (t, *J* = 7.5 Hz, 1H), 6.96 (t, *J* = 7.5 Hz, 1H), 4.78 (s, 2H), 3.67 (s, 3H), 2.96 (s, 3H), 2.89 (m, 2H), 2.51 (m, 2H), 2.45 (s, 3H). LCMS (ES) *m/e* 389 (M + H)⁺. Anal. (C₂₃H₂₄N₄O₂·1.0H₂O) C, H, N.

(E)-N-Methyl-3-(7-oxo-5,6,7,8-tetrahydro-1,8-naphthyridin-3-yl)-N-(1,2,7-trimethyl-1H-indol-3-ylmethyl)acrylamide (32). According to the procedure of compound **21**, except substituting 3-(methylaminomethyl)-1,2,7-dimethylindole (**28**) (0.57 g, 2.8 mmol) for 1-methyl-2-(methylamino-

methyl)indole, the title compound (0.78 g, 70%) was prepared as an off-white solid. LC-MS (ES) *m/e* 403 (M + H)⁺. Anal. (C₂₄H₂₆N₄O₂·2.75 H₂O) C, H, N.

X-ray Crystallography. Crystals of the *E. coli* FabI/NAD⁺ complex with **29** were obtained using the same methods and conditions as those reported earlier.³⁷ X-ray diffraction data to 2.33 Å resolution were collected on a flash cooled crystal at the Brookhaven National Laboratories National Synchrotron Light Source. Data were integrated, scaled, and merged with the program HKL2000.³⁸ Statistics on data quality and refinement are shown in Table 2. The structure was solved by difference Fourier methods using the *E. coli* FabI-NAD⁺-trichosan structure³⁷ as the starting model. The program CNX³⁸ was used for refinement and the program O⁴⁰ was used for graphic display and model building. Each asymmetric unit contains one FabI dimer with one NAD⁺ and one molecule of inhibitor per FabI monomer. Portions of the flipping loop³⁷ are disordered (residues 196 and 199–200 in monomer 1 and residues 195–196 and 200–205 in monomer 2). The electron density for the cofactor and inhibitor unambiguously indicated the position of the molecules although density for the inhibitors is less clear and B-factors for the inhibitor molecules are high at 84Å² (see Supporting Information). The structure was validated with the program PROCHECK⁴¹ and has excellent stereochemistry. Figures were made using the program PYMOL⁴² and the program MOLMOL.⁴³ The accession code for **29** is 1MFP.

***S. aureus* FabI Enzyme Inhibition Assay.** Assays are carried out in half-area, 96-well microtiter plates. Compounds are evaluated in 150-μL assay mixtures containing 100 mM NaADA (ADA = *N*-[2-acetamido]-2-iminodiacetic acid), pH 6.5, 4% glycerol, 25 μM crotonoyl-ACP, 50 μM NADPH, and an appropriate dilution of *S. aureus* FabI (approximately 20 nM). Inhibitors are typically varied over the range of 0.01–10 μM. The consumption of NADPH is monitored for 20 min at 30 °C by following the change in absorbance at 340 nm. Initial velocities are estimated from a linear fit of the progress curves. IC₅₀'s were estimated from a fit of the initial velocities to a standard, four-parameter model ($v = \text{range}/(1 + [I]/IC_{50}) + \text{background}$) and are typically reported as the mean ± SD of duplicate determinations. Triclosan, a commercial antibacterial agent and inhibitor of FabI, was included in all assays as a positive control.

***H. influenzae* FabI Enzyme Inhibition Assay.** Assays are carried out in half-area, 96-well microtiter plates. Compounds are evaluated in 150-μL assay mixtures containing 100 mM MES, 51 mM diethanolamine, 51 mM triethanolamine, pH 6.5 (MES = 2-(*N*-morpholino)ethanesulfonic acid), 4% glycerol, 25 μM crotonoyl-ACP, 50 μM NADH, and an appropriate dilution of *H. influenzae* FabI (approximately 20 nM). Inhibitors were typically varied over the range of 0.01–10 μM. The consumption of NADH was monitored for 20 min at 30 °C by following the change in absorbance at 340 nm. Initial velocities were estimated from an exponential fit of the nonlinear progress curves. IC₅₀'s were estimated from a fit of the initial velocities to a standard, 4-parameter model, and are typically reported as the mean ± SD of duplicate determinations. A proprietary lead compound was included in all assays as a positive control.

***E. coli* FabI Enzyme Inhibition Assay.** Assays were carried out in half-area, 96-well microtiter plates. Compounds were evaluated in 150-μL assay mixtures containing 100 mM NaADA, pH 6.5 (ADA = *N*-[2-acetamido]-2-iminodiacetic acid), 4% glycerol, 0.25 mM crotonoyl-CoA, 50 μM NADH, and an appropriate dilution of *E. coli* FabI. Inhibitors were typically varied over the range of 0.01–10 μM. The consumption of NADH was monitored for 20 min at 30 °C by following the change in absorbance at 340 nm. Initial velocities were estimated from an exponential fit of the nonlinear progress curves represented by the slope of the tangent at *t* = 0 min. IC₅₀'s were estimated from a fit of the initial velocities to a standard, 4-parameter model and are typically reported as the mean ± SD of duplicate determinations. Triclosan was included in all assays as a positive control.

***S. aureus* FabK Enzyme Inhibition Assay.** Assays were carried out in half-area, 96-well microtiter plates. Compounds were evaluated in 100 μL assay mixtures containing MDT buffer (100 mM MES, 51 mM diethanolamine, 51 mM triethanolamine) pH 7.5 with 100 mM NH₄Cl, 4% glycerol, 25 μM crotonoyl-ACP, 50 μM NADH, and 1.5 nM *S. pneumoniae* FabK. Inhibitors were tested at either a single concentration of 30 μM or varied over the range of 0.01–10 μM. The consumption of NADH was monitored for 5 min at 30 °C by following the change in absorbance at 340 nm. Initial velocities were estimated from an exponential fit of the nonlinear progress curves represented by the slope of the tangent at *t* = 0 min. IC₅₀'s were estimated from a fit of the initial velocities to a standard, four-parameter model and are typically reported as the mean ± standard deviation (SD) of duplicate determinations.

Antimicrobial Activity Assay. Whole-cell antimicrobial activity was determined by broth microdilution using the National Committee for Clinical Laboratory Standards (NCCLS) recommended procedure, Document M7-A4, "Methods for Dilution Susceptibility Tests for Bacteria that Grow Aerobically". Compounds were tested in serial 2-fold dilutions ranging from 0.06 to 64 μg/mL. For some compounds, a lower dilution scheme was used. The minimum inhibitory concentration (MIC) was determined as the lowest concentration of compound that inhibited visible growth. A mirror reader was used to assist in determining the MIC endpoint.

Acknowledgment. We thank John Broskey and Leroy L. Voelker of the Antiinfectives Department for cytotoxicity data, Robert I. Jepras of the Computational and Structural Sciences Department for liposome lysis data, Priscilla Offen of the Physical and Structural Chemistry Department for NMR studies, Stone D. Shi and Mark E. Hemling of the Physical and Structural Chemistry Department for high resolution mass spectra, and Ward W. Smith for preparing X-ray density figures. We also thank the staff at beamline X12-C of the Biology Department Single-Crystal Diffraction Facility at the National Synchrotron Light Source (NSLS) of Brookhaven National Laboratory. The NSLS facility is supported by the U.S. Department of Energy, Offices of Health and Environmental Research and of Basic Energy Sciences under prime contract DE-AC02-98CH10886, by the National Science Foundation, and by National Institutes of Health Grant 1P41 RR12408-01A1.

Supporting Information Available: A table of crystallographic data acquisition and refinement statistics for inhibitor **29** bound to *E. coli* FabI/NAD⁺, density figures for inhibitor **29** bound to *E. coli* FabI/NAD⁺. This material is available free of charge via the Internet at <http://pubs.acs.org>.

References

- Bax, R.; Mullan, N.; Verhoef, J. The millennium bugs – the need for and development of new antibacterials. *Int. J. Antimicrob. Agents* **2000**, *16*, 51–59.
- Setti, E. L.; Quattrocchio, L.; Micetich, R. G. Current approaches to overcome bacterial resistance. *Drugs Future* **1997**, *22*, 271–284.
- Chu, D. T. W.; Plattner, J. J.; Katz, L. New directions in antibacterial research. *J. Med. Chem.* **1996**, *39*, 3853–3874.
- Pearson, H. 'Superbug' hurdles key drug barrier. *Nature* **2002**, *418*, 469.
- Payne, D. J.; Warren, P. V.; Holmes, D. J.; Ji, Y. D.; Lonsdale, J. T. Bacterial fatty acid biosynthesis: a genomics driven target for antibacterial drug discovery. *Drug Discovery Today* **2001**, *6*, 537–544.
- Heath, R. J.; White, S. W.; Rock, C. O. Lipid biosynthesis as a target for antibacterial agents. *Prog. Lipid Res.* **2001**, *40*, 467–497.
- Campbell, J. W.; Cronan, J. E., Jr. Bacterial fatty acid biosynthesis: targets for antibacterial drug discovery. *Annu. Rev. Microbiol.* **2001**, *55*, 305–332.

- (8) Heath, R. J.; Rock, C. O. Enoyl-acyl carrier protein reductase (*fabI*) plays a determinant role in completing cycles of fatty acid elongation in *Escherichia coli*. *J. Biol. Chem.* **1995**, *270*, 26538–26542.
- (9) Bergler, H.; Fuchsbichler, S.; Högenauer, G.; Turnowsky, F. The enoyl-[acyl-carrier-protein] reductase (FabI) of *Escherichia coli*, which catalyzes a key regulatory step in fatty acid biosynthesis, accepts NADH and NADPH as cofactors and is inhibited by palmitoyl-CoA. *Eur. J. Biochem.* **1996**, *242*, 689–694.
- (10) Heath, R. J.; Li, J.; Roland, G. E.; Rock, C. O. Inhibition of the *Staphylococcus aureus* NADPH-dependent enoyl-acyl carrier protein reductase by triclosan and hexachlorophene. *J. Biol. Chem.* **2000**, *275*, 4654–4659.
- (11) Rozwarski, D. A.; Grant, G. A.; Barton, D. H. R.; Jacobs, W. R., Jr.; Sacchettini, J. C. Modification of the NADH of the isoniazid target (InhA) from *Mycobacterium tuberculosis*. *Science* **1998**, *279*, 98–102.
- (12) Baldock, C.; Rafferty, J. B.; Sedelnikova, S. E.; Baker, P. J.; Stuitje, A. R.; Slabas, A. R.; Hawkes, T. R.; Rice, D. W. A mechanism of drug action revealed by structural studies of enoyl reductase. *Science* **1996**, *274*, 2107–2110.
- (13) Baldock, C.; de Boer, G.-J.; Rafferty, J. B.; Stuitje, A. R.; Rice, D. W. Mechanism of action of diazaborines. *Biochem. Pharm.* **1998**, *55*, 1541–1550.
- (14) Levy, C. W.; Baldock, C.; Wallace, A. J.; Sedelnikova, S.; Viner, R. C.; Clough, J. M.; Stuitje, A. R.; Slabas, A. R.; Rice, D. W.; Rafferty, J. B. A study of the structure–activity relationship for diazaborine inhibition of *Escherichia coli* enoyl-ACP reductase. *J. Mol. Biol.* **2001**, *309*, 171–180.
- (15) McMurry, L. M.; Oethinger, M.; Levy, S. B. Triclosan targets lipid synthesis. *Nature* **1998**, *394*, 531–532.
- (16) Heath, R. J.; Yu, Y.-T.; Shapiro, M. A.; Olson, E.; Rock, C. O. Broad spectrum antimicrobial biocides target the FabI component of fatty acid synthesis. *J. Biol. Chem.* **1998**, *273*, 30316–30320.
- (17) Levy, C. W.; Roujeinikova, A.; Sedelnikova, S.; Baker, P. J.; Stuitje, A. R.; Slabas, A. R.; Rice, D. W.; Rafferty, J. B. Molecular basis of triclosan activity. *Nature* **1999**, *398*, 383–384.
- (18) McMurry, L. M.; McDermott, P. F.; Levy, S. B. Genetic evidence that InhA of *Mycobacterium smegmatis* is a target for triclosan. *Antimicrob. Agents Chemother.* **1999**, *43*, 711–713.
- (19) Heath, R. J.; Rock, C. O. A triclosan-resistant bacterial enzyme. *Nature* **2000**, *406*, 145–146.
- (20) Heath, R. J.; Su, N.; Murphy, C. K.; Rock, C. O. The enoyl-[acyl-carrier-protein] reductases FabI and FabL from *Bacillus subtilis*. *J. Biol. Chem.* **2000**, *275*, 40128–40133.
- (21) Heering, D. A.; Chan, G.; DeWolf, W. E., Jr.; Fosberry, A. P.; Janson, C. A.; Jaworski, D. D.; McManus, E.; Miller, W. H.; Moore, T. D.; Payne, D. J.; Qiu, X.; Rittenhouse, S. F.; Slater-Radosti, C.; Smith, W.; Takata, D. T.; Vaidya, K. S.; Yuan, C. C. K.; Huffman, W. F. 1,4-Disubstituted imidazoles are potential antibacterial agents functioning as inhibitors of enoyl acyl carrier protein reductase (FabI). *Bioorg. Med. Chem. Lett.* **2001**, *11*, 2061–2065.
- (22) Seefeld, M. A.; Miller, W. H.; Newlander, K. A.; Burgess, W. J.; Payne, D. J.; Rittenhouse, S. F.; Moore, T. D.; DeWolf, W. E., Jr.; Keller, P. M.; Qiu, X.; Janson, C. A.; Vaidya, K.; Fosberry, A. P.; Smyth, M. G.; Jaworski, D. D.; Slater-Radosti, C.; Huffman, W. F. Inhibitors of bacterial enoyl acyl carrier protein reductase (FabI): 2,9-disubstituted 1,2,3,4-tetrahydropyrido[3,4-b]indoles as potential antibacterial agents. *Bioorg. Med. Chem. Lett.* **2001**, *11*, 2241–2244.
- (23) Miller, W. H.; Seefeld, M. A.; Newlander, K. A.; Uzinskas, I. N.; Burgess, W. J.; Heering, D. A.; Yuan, C. C. K.; Head, M. S.; Payne, D. J.; Rittenhouse, S. F.; Moore, T. D.; Pearson, S. C.; Berry, V.; DeWolf, W. E., Jr.; Keller, P. M.; Polizzi, B. J.; Qiu, X.; Janson, C. A.; Huffman, W. F. Discovery of aminopyridine-based inhibitors of bacterial enoyl-ACP reductase (FabI). *J. Med. Chem.* **2002**, *45*, 3246–3256.
- (24) Heck, R. F. Palladium-catalyzed vinylation of organic halides. *Org. Reactions* **1982**, *27*, 345–390.
- (25) Murakami, Y.; Sunamoto, J.; Kinuwaki, S.; Honda, H. Synthesis of Organic Phosphates. III. Synthesis and Properties of 2-amino-3-pyridylmethyl and 2-chloro-3-pyridylmethyl Phosphates. *Bull. Chem. Soc. Jpn.* **1973**, *46*, 2187–2190.
- (26) James, P. N.; Snyder, H. R. *Organic Syntheses*; Rabjohn, Norman, Ed.; Wiley: New York, 1963; Collect. Vol. IV, pp 539–542.
- (27) The apparent K_i value was calculated from the estimated IC_{50} value assuming competitive inhibition with the substrate crotonoyl-ACP. However, since detailed mechanistic studies could not be done, due to the low K_m of the substrate and limitations in the sensitivity of the assay, the true K_i value could not be determined.
- (28) The *E. coli* FabI assay used crotonoyl-CoA, rather than the natural substrate crotonoyl-ACP. See the Experimental Section for details.
- (29) Payne, D. J.; Miller, W. H.; Berry, V.; Brosky, J.; Burgess, W. J.; Chen, E.; DeWolf, W. E., Jr.; Fosberry, A. P.; Greenwood, R.; Head, M. S.; Heering, D. A.; Janson, C. A.; Jaworski, D. D.; Keller, P. M.; Manley, P. J.; Moore, T. D.; Newlander, K. A.; Pearson, S.; Polizzi, B. J.; Qiu, X.; Rittenhouse, S. F.; Slater-Radosti, C.; Salyers, K. L.; Seefeld, M. A.; Smyth, M. G.; Takata, D. T.; Uzinskas, I. N.; Vaidya, K.; Wallis, N. G.; Winram, S. B.; Yuan, C. C. K.; Huffman, W. F. Discovery of a novel and potent class of FabI directed antibacterial agents. *Antimicrob. Agents Chemother.* **2002**, *46*, 3118–3124.
- (30) Heath, R. J.; Rubin, J. R.; Holland, D. R.; Zhang, E.; Snow, M. E.; Rock, C. O. Mechanism of triclosan inhibition of bacterial fatty acid synthesis. *J. Biol. Chem.* **1999**, *274*, 11110–11114.
- (31) Ward, W. H. J.; Holdgate, G. A.; Rowsell, S.; McLean, E. G.; Pauptit, R. A.; Clayton, E.; Nichols, W. W.; Colls, J. G.; Minshull, C. A.; Jude, D. A.; Mistry, A.; Timms, D.; Camble, R.; Hales, N. J.; Britton, C. J.; Taylor, I. W. F. Kinetic and structural characteristics of the inhibition of enoyl (acyl carrier protein) reductase by triclosan. *Biochemistry* **1999**, *38*, 12514–12525.
- (32) Marcinkeviciene, J.; Jiang, W.; Kopcho, L. M.; Locke, G.; Luo, Y.; Copeland, R. A. Enoyl-ACP reductase (FabI) of *Haemophilus influenzae*: steady-state kinetic mechanism and inhibition by triclosan and hexachlorophene. *Arch. Biochem. Biophys.* **2001**, *390*, 101–108.
- (33) Fan, F.; Yan, K.; Wallis, N. G.; Reed, S.; Moore, T. D.; Rittenhouse, S. F.; DeWolf, W. E., Jr.; Huang, J.; McDevitt, D.; Miller, W. H.; Seefeld, M. A.; Newlander, K. A.; Jakas, D. R.; Head, M. S.; Payne, D. J. Defining and combating the mechanisms of triclosan resistance in clinical isolates of *Staphylococcus aureus*. *Antimicrob. Agents Chemother.* **2002**, *46*, 3343–3347.
- (34) Suller, M. T. E.; Russell, A. D. Triclosan and antibiotic resistance in *Staphylococcus aureus*. *J. Antimicrob. Chemother.* **2000**, *46*, 11–18.
- (35) Liu, B.; Wang, Y.; Fillgrove, K. L.; Anderson, V. E. Triclosan inhibits enoyl-reductase of type I fatty acid synthase in vitro and is cytotoxic to MCF-7 and SKBr-3 breast cancer cells. *Cancer Chemother. Pharmacol.* **2002**, *49*, 187–193.
- (36) Mechanistic studies with **29** and *S. aureus* FabI showed mixed inhibition versus its cosubstrate NADPH and displayed inhibition parameters consistent with a preference for binding to the cofactor-bound form of the enzyme; Walter E. DeWolf, unpublished results.
- (37) Qiu, X.; Janson, C. A.; Court, R. I.; Smyth, M. G.; Payne, D. J.; Abdel-Meguid, S. S. Molecular basis for triclosan activity involves a flipping loop in the active site. *Prot. Sci.* **1999**, *8*, 2529–2532.
- (38) Otwinowski, Z.; Minor, W. Processing of X-ray Diffraction Data Collected in Oscillation Mode. *Methods in Enzymology*; Carter, C. W., Jr., Sweet, R. M., Eds.; Academic Press: New York, 1997; Volume 276: Macromolecular Crystallography, part A, pp 307–326.
- (39) Brünger, A. T.; Adams, P. D.; Clore, G. M.; DeLano, W. L.; Gros, P.; Grosse-Kunstleve, R. W.; Jiang, J.-S.; Kuszewski, J.; Nilges, M.; Pannu, N. S.; Read, R. J.; Rice, L. M.; Simonson, T.; Warren, G. L. Crystallography & NMR System: A new software suite for macromolecular structure determination. *Acta Crystallogr.* **1998**, *D54*, 905–921.
- (40) Jones, T. A.; Zou, J. Y.; Cowan, S. W.; Kjeldgaard, M. Improved methods for binding protein models in electron density maps and the location of errors in these models. *Acta Cryst.* **1991**, *A47*, 110–119.
- (41) Laskowski, R. A.; MacArthur, M. W.; Moss, D. S.; Thornton J. M. PROCHECK: a program to check the stereochemical quality of protein structures. *J. Appl. Crystallogr.* **1993**, *26*, 283–291.
- (42) DeLano, W. L. The PyMOL Molecular Graphics System 2002, DeLano Scientific, San Carlos, CA.
- (43) Koradi, R.; Billeter, M.; Wütrich, K. MOLMOL: A program for display and analysis of macromolecular structures. *J. Mol. Graphics* **1996**, *14*, 51–55.